Experimental Eye Research 209 (2021) 108620

Contents lists available at ScienceDirect

Experimental Eye Research

journal homepage: www.elsevier.com/locate/yexer

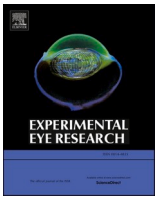

Modeling the effects of glaucoma surgery on intraocular pressure

Nicholas Farrar [a], David B. Yan [b], Mark Johnson [a,c,d,*]

[a] Department of Biomedical Engineering, Northwestern University, 2145 Sheridan Road, E310, Evanston, IL 60208, USA
[b] Department of Ophthalmology and Vision Sciences, University of Toronto, 340 College Street, Suite 400, Toronto, ON. M5T 3A9, Canada
[c] Department of Mechanical Engineering, Northwestern University, 2145 Sheridan Road, Room B224, Evanston, IL 60208, USA
[d] Department of Ophthalmology, Northwestern University, 645 N. Michigan Ave. Suite 440, Chicago, IL 60611, USA

ARTICLE INFO

Keywords:
Model
MIGS
Stents
Trabeculotomy

ABSTRACT

Minimally invasive glaucoma surgeries (MIGS) offer an effective way to lower intraocular pressure without inducing extensive trauma to the anterior segment. In order to predict their efficacy, an analytical model of the conventional aqueous humor outflow pathway is developed using a resistor network. The model describes outflow through the normal eye and allows for the effects of geometric changes in the outflow pathway as IOP changes. By selectively removing these resistors, the model can be used to examine and predict the outcomes of several surgical procedures currently used to treat glaucoma. Treatments examined include traditional trabeculectomy, several ab interno methods for trabeculotomy and trabeculectomy, as well as recently developed trabecular stents that bypass the trabecular meshwork and dilate Schlemm canal. The model's predictions for the efficacy of these procedures generally matched well with the efficacy determined in experimental studies, although it tended to somewhat overestimate the efficacy of these procedures. Matching the model to experimental data indicated that a partial trabeculotomy substantially increases flow to collector channels within that region and approximately 1.5 clock hours past the ends of the trabeculotomized region. Similarly, trabecular bypass stents substantially increase flow to collector channels up to 1.5 clock hours past the open ends of the stent. The resistor model we have developed can be used to predict the efficacy of a variety of MIGS procedures. Circumferential flow in Schlemm canal extends the efficacy of MIGS, but this effect is limited to a few clock hours.

1. Introduction

Lowering of intraocular pressure (IOP) is the only established treatment for glaucoma (Weinreb et al., 2014), and pharmacological treatment is usually the first choice for medical therapy. However, for many patients, surgery is required to sufficiently lower IOP so as to either slow or stop the disease process. Traditional glaucoma surgery creates a full thickness passageway between the anterior chamber to the subconjunctival or sub-Tenon's space, either by partial thickness dissection of the scleral (in a trabeculectomy) or insertion of a silicon tube connected to an outer plate (in a tube shunt). The extensive trauma to the anterior segment and relatively uncontrolled rate of fluid flow directly to the outside of the eye is associated with a high rate of post-operative complications (Gedde et al., 2012). There is a desire to adopt procedures that minimize such trauma including ab interno trabeculotomy, small shunts placed into Schlemm canal, or localized laser ablation (Kaplowitz et al., 2014; Richter and Coleman, 2016). Predicting the potential success of such therapies would aid in their development and adoption.

The extent to which IOP is elevated over episcleral venous pressure is determined primarily by the rate at which aqueous humor is produced by the ciliary body and by the outflow resistance generated as aqueous humor passes through the conventional outflow pathway[1]. This outflow resistance is generated as the aqueous humor flows sequentially through 1) trabecular meshwork, 2) inner wall of Schlemm canal, 3) Schlemm canal itself, 4) collector channels, 5) aqueous veins, and finally 6) anastomosing back into the episcleral venous system. Under normal conditions, approximately half of the flow resistance is generated by the trabecular meshwork and inner wall of Schlemm canal, and half by the collector channels and aqueous veins, with little flow resistance or pressure drop occurring in Schlemm canal itself (Rosenquist et al.,

* Corresponding author. Department of Biomedical Engineering, Northwestern University, 2145 Sheridan Road, E310, Evanston, IL 60208, USA.
E-mail address: m-johnson2@northwestern.edu (M. Johnson).

[1] Approximately 10% (range: 0–14%) of aqueous humor outflow passes through an alternate pathway known as the unconventional outflow pathway (Johnson et al., 2017). We do not further consider that pathway here.

https://doi.org/10.1016/j.exer.2021.108620
Received 29 January 2021; Received in revised form 13 April 2021; Accepted 10 May 2021
Available online 25 May 2021

Abbreviations and acronyms

IOP	intraocular pressure
TM	trabecular meshwork and inner wall of Schlemm canal
SC	Schlemm canal
CC	collector channel or aqueous vein
GATT	Gonioscopy-assisted transluminal trabeculotomy
MIGS	minimally invasive glaucoma surgery

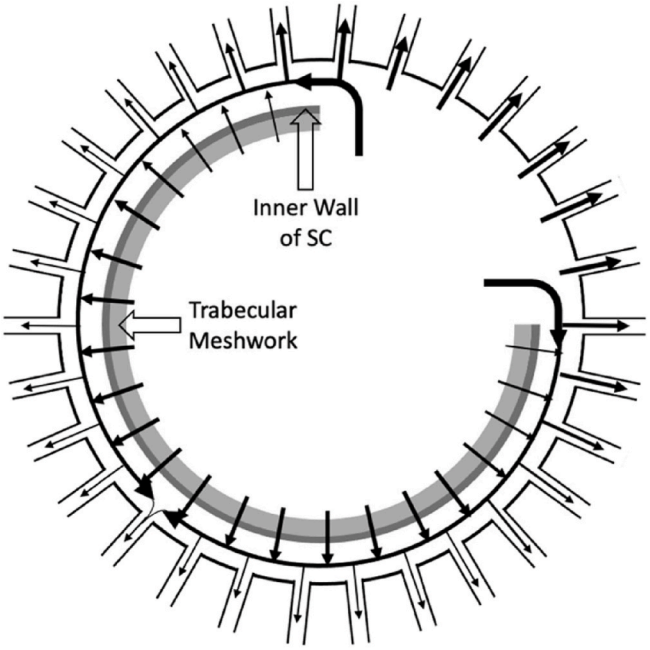

Fig. 1. Schematic of aqueous humor outflow pathway after 3-h trabeculotomy showing flow distribution (more flow is indicated by thicker arrows).

1989). The elevated IOP characteristic of glaucoma is thought to be caused primarily by increased flow resistance in the trabecular meshwork and inner wall of Schlemm canal (Johnson, 2006).

Glaucoma surgery can change the path taken by aqueous humor through the conventional outflow pathway. Normally, aqueous humor flows through the trabecular meshwork and inner wall of Schlemm canal, with some regions permitting high flow and others permitting less flow (de Kater et al., 1989). Aqueous humor then briefly passes through Schlemm canal and drains through the nearest collector channel. As shown in Fig. 1, a 3-h trabeculectomy where only the trabecular meshwork was removed would significantly alter this flow distribution. With the aqueous humor now having free access to Schlemm canal, most of the flow will enter the canal through the trabeculectomy and drain through the exposed collector channels. Intuitively, if this free access to collector channels removed the vast majority of the outflow resistance, IOP would drop close to episcleral venous pressure with a localized removal of the trabecular meshwork. However, this is not observed in surgical studies that aim to bypass the trabecular meshwork, and other components of the conventional outflow pathway are likely to play a greater role in generating outflow resistance when the system has been altered surgically. A significant fraction of the flow may travel through Schlemm canal and distribute itself among the other collector channels, with the collector channels closest to the trabeculectomy getting the bulk of this flow.

Without a model, predicting the flow distribution and the resulting

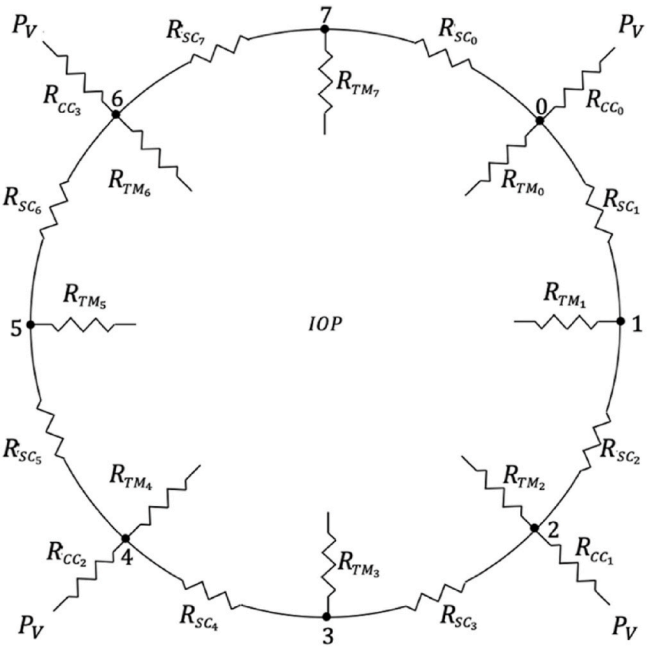

Fig. 2. Example of resistor network with N = 4 CCs and M = 2 SC resistors between each pair of collector channels. Numbers represent Schlemm canal nodes. R_{TMi} and R_{SCi} represent the resistances of the TM and SC resistors at a given node. R_{CCk} represents the resistance of the kth CC resistor. IOP and P_V respresent intraocular pressure and episcleral venous pressure, respectively.

IOP reduction following MIGS would be challenging even if the flow resistance of all components of this network were constant. But as IOP changes, the flow resistance of Schlemm canal, collector channels and aqueous veins also change (Johnstone and Grant, 1973; Rosenquist et al., 1989). We developed a simple resistor model of the aqueous humor outflow pathway that allows for predictions of the effect of various surgical interventions on outflow resistance (see Supplementary Data for software implementation). Our results show that while even a small opening into Schlemm canal can significantly lower IOP, the flow resistance of the collector channels and aqueous veins is sufficiently high as to generate significant circumferential flow through Schlemm canal that limits the potential IOP reduction achievable by procedures that open limited aspects of Schlemm canal. This model could aid in the future development and refinement of angle-based MIGS procedures to optimize their efficacy in reducing IOP. A program implementing our model is currently online and can be accessed at Aqueous Humor Outflow Model.

2. Methods

2.1. Baseline model of eye

The conventional aqueous outflow pathway is modeled as a network of flow resistors. Three different types of flow resistors are defined, representing the (i) trabecular meshwork and inner wall of Schlemm canal (TM), (ii) Schlemm canal (SC), and (iii) the collector channels and aqueous veins (CCs). For a given IOP or aqueous humor flow rate (Q_T), the pressure at each node in the system is determined using Kirchoff's laws for current (flow) and voltage (pressure).

The model of the outflow pathway allows for a variable number of resistors in the network. One resistor is assigned for each of N CCs. Within Schlemm canal, M resistors were placed evenly between every two CCs. The TM is represented as having $N \times M$ resistors. The resulting network has $N \times M$ nodes in SC with the pressure and flow of each of those nodes designated as P_i and Q_i, with i varying from 1 to $N \times M$. An example of the resulting resistor network model with $N = 4$ and $M = 2$ is shown in Fig. 2.

The actual resistor network used to perform our baseline simulations is much larger. We used N = 30 as a typical number of CCs in the human eye (Moses, 1977). The number of SC resistors between CCs ($M = 40$) was chosen in order to optimize the accuracy of the model and minimize computational cost. Increasing M past 40 yielded minimal increases in accuracy, but significantly increased computational expense.

The resistance of each resistor in the network is designated as $R_{i,j}$ where i and j are the nodes in the network connected by the resistor. Node 0 is IOP and node $N \times M + 1$ is episcleral venous pressure (P_v). Nodes 1 to $N \times M$ are in Schlemm canal. $R_{i,j}$ is infinite for any two nodes not directly connected to one another. The $N \times M$ resistors modeling the trabecular meshwork and inner wall endothelium each have a resistance of

$$R_{0,i} = N\,M\,R_{TM} \tag{1}$$

where R_{TM} is the total resistance of the trabecular meshwork and inner wall endothelium with i varying from 1 to $N \times M$.

Schlemm canal is modeled as a compliant, porous duct that is elliptical in cross-section (Ethier et al., 2004). For such a duct with width W and height h, the pressure gradient is found as:

$$\frac{dP}{dx} = -\frac{64\mu Q(x)}{\pi W h^3(x)} \tag{2}$$

where x is distance from the midpoint of the canal between two CCs, Q (x) is the flow rate and μ is the viscosity of the aqueous humor (White and Corfield, 2006). By assuming that the height varies linearly between adjacent SC nodes and integrating equation (2) from the i^{th} node to the j^{th} node (see Supplementary Data), the resistance of a given SC resistor is then found as:

$$R_{i,j} = \frac{|P_j - P_i|}{Q(x)} = \frac{32\mu(h_i + h_j)\Delta x}{\pi\, W\, h_i^2\, h_j^2} \tag{3}$$

where Δx is the distance between adjacent SC nodes and i and j are the number of the adjacent nodes that the resistor connects.

The height of the canal is assumed to vary as a function of the pressure drop across the TM. Two regimes are considered, depending on whether the canal is being held open primarily by tension in the trabecular meshwork, or by compression of the septae in Schlemm canal (Hoffmann and Dumitrescu, 1971; Johnson and Kamm, 1983). When the canal is held open by the tension in the trabecular meshwork, the height is assumed to vary linearly with the pressure drop ($IOP - P_i$) across the trabecular meshwork and inner wall of Schlemm canal:

$$h_i = h_0\left(1 - \frac{IOP - P_i}{E_{TM}}\right) \tag{4}$$

where h_0 is the undeformed height of the canal, P_i is the pressure in SC, E_{TM} is the modulus of elasticity of the trabecular meshwork and i = 1 to N^*M.

Complete canal collapse at higher pressure drops across the inner wall is prevented by support structures in the canal known as septae (Hoffmann and Dumitrescu, 1971). The septae can be thought of as beams between the inner and outer walls of Schlemm canal whose compression opposes canal collapse. The relation governing canal height in this regime is determined by an order of magnitude analysis (see Appendix A) to be

$$h_i = h_s\left[\frac{K_S}{(IOP - P_i)}\right]^{1/3} \tag{5}$$

where h_s is the height of Schlemm canal at which the septae begin to oppose canal compression and K_S is a stiffness parameter characterizing the septae. Recognizing that canal height given by equations (4) and (5) must be the same when $h_i = h_s$, we find that K_s is not an independent parameter and is calculated as

Table 1
Baseline model parameters.

Parameter	Description	Value	Source
N	Number of CCs	30	Moses (1977)
M	Number of SC resistors/nodes between adjacent CCs	40	Optimal resolution
Q_T	Conventional flowrate of aqueous humor	2 μL/min	Brubaker (1982)
R_{TM}	Overall resistance of TM	2 mmHg/μL/min	Rosenquist et al. (1989)
μ	Viscosity of aqueous humor	0.007 g/cm/sec	Moses (1977)
W	Width of SC	230 μm	Zhou and Smedley (2006)
h_0	Undeformed height of SC	20 μm	Zhou and Smedley (2006)
h_s	Undeformed height of septae	3.0 μm	Least-squares fit
E_{TM}	Young's modulus of TM	13 mmHg	Least-squares fit
K_S	Stiffness of septae	11.05 mmHg	Equation (6)

$$K_s = E_{TM}\left(1 - \frac{h_s}{h_0}\right) \tag{6}$$

The values of the parameters h_s, E_{TM}, and K_S were determined by a best fit of the model to a pressure-resistance curve for enucleated human eyes (Brubaker, 1975) using the parameters in Table 1 with $P_v = 0$ mmHg.

The N resistors modeling collector channels were each assumed to have the same flow resistance:

$$R_{i^*M,(N^*M+1)} = N\,R_{CC} \tag{7}$$

where R_{CC} is the total resistance of all the CCs and i = 1 to N. Rosenquist et al. (1989) measured outflow resistance after complete trabeculotomy (i.e. only CC resistance remaining) at IOP = 7 mmHg and IOP = 25 mmHg, and we used their values to estimate R_{cc} with the following relationship:

$$R_{CC} = 2.03\frac{mmHg}{\mu L/min} - (0.033\ min/\mu L)\ (IOP\ -\ P_v) \tag{8}$$

The resistances R_{ij} were used to find the conductances G_{ij} (the conductance is the inverse of the resistance such that $G_{ij} = 1/R_{ij}$). Using this conductance matrix, the following linear system of equations can be constructed using Kirchoff's current and voltage laws and solved to find the pressure distribution in SC

$$G(\vec{p}^{(k)})\,\vec{p}^{(k+1)} = \vec{q} \tag{9}$$

where $G(\vec{p})$ is the matrix of conductances, $\vec{p}$ is the pressure vector $[p_0 - P_v, p_1 - P_v, \ldots, p_{NM-1} - P_v, IOP - P_v]^T$, and $\vec{q}$ is the flow rate vector $[0, 0, \ldots, 0, Q_T]^T$. When IOP is specified instead of Q_T, IOP is moved to the righthand side of the equation, so that the last element of $\vec{p}$ is removed, and $\vec{q}$ becomes $[-(IOP - P_v)/R_{0,0},\ -(IOP - P_v)/R_{0,1},\ \ldots,\ -(IOP - P_v)/R_{0,NM-1}]$. Note that the conductance matrix is a function of the pressure vector. This has two consequences. Before the system can be solved the first time, an initial guess for the pressure vector must be made. The value used for this guess has essentially no effect on the final result, but does affect computation time, so it is most efficient to select a reasonable guess. The initial guess used for simulations where IOP is specified (constant pressure mode) is what the pressure in the canal would be assuming that SC offers no resistance to fluid flow, yielding

$$P_{guess} = IOP\left(\frac{R_{CC}}{R_{TM} + R_{CC}}\right) \tag{10}$$

Since this value is dependent on IOP, an initial guess is also needed for IOP when only Q_T is specified (constant flow mode). This guess is

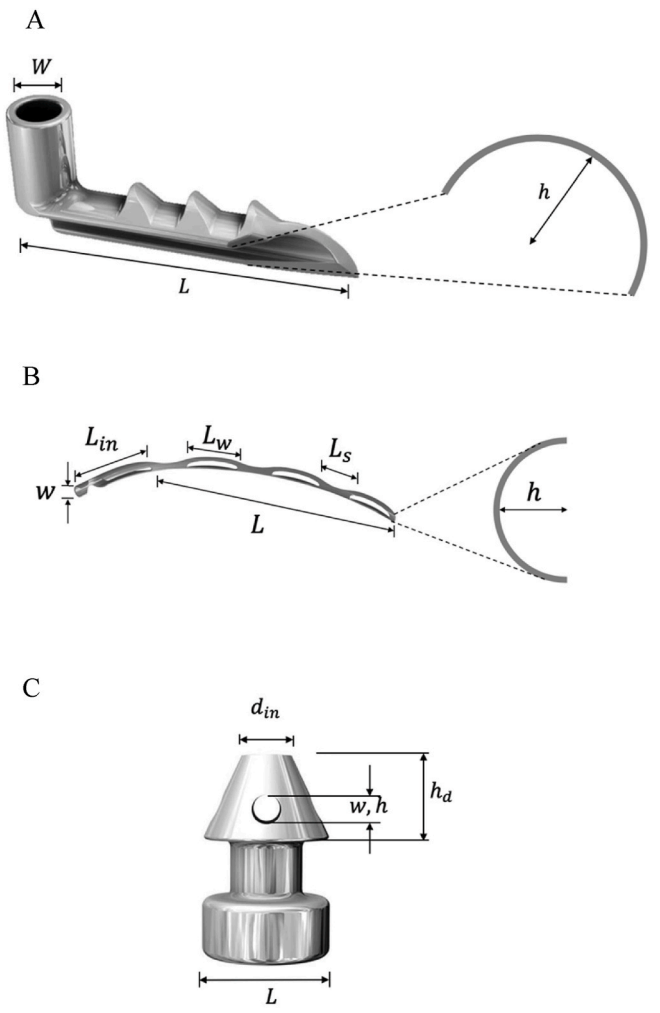

Fig. 3. Stents modeled in study annotated with dimensions given Table 2 (A) First-generation iStent (Magazine, 2018) (B) 8 mm Hydrus Microstent (Gulati et al., 2013), (C) iStent *inject* (Glaukos).

$$IOP_{guess} = Q_T(R_{TM} + R_{CC}) \tag{11}$$

The other consequence of G being a function of $\vec{p}$ is that the linear system in equation (9) must be solved iteratively, recalculating the conductance matrix with each new pressure vector. The indices k and $(k+1)$ refer to the k^{th} and $(k+1)^{th}$ iterations of the solution, respectively. Equation (9) is repeatedly solved until $\vec{p}$ converges on a value. The metric used for determining convergence is

$$Residual = \frac{1}{IOP}\sqrt{\frac{\sum_{i=0}^{NM-1}\left(p_i^{(k+1)} - p_i^{(k)}\right)^2}{NM}} \tag{12}$$

and convergence is said to have occurred when $Residual < 10^{-4}$. For most cases, Gaussian elimination is used to solve the system; however, occasionally when the canal is in transition between the two height regimes, Gaussian elimination is unable reach a stable solution, and in such cases, the iterative Gauss-Seidel method is used.

The model parameters used for the baseline model describing the normal human eye are shown in Table 1. The flow rate chosen, Q = 2 μl/min, is the flow through the conventional outflow pathway, and does not include flow through the unconventional pathway or any posteriorly directed flow.

Table 2
Dimensions of stents.

DEVICE	Description	Value	Source
iStent			
L	Length of the device in SC	1 mm	Hunter et al. (2014)
w	Width of the device	120 μm	Katz et al. (2015)
h	Height of device in SC	60 μm	Katz et al. (2015)
8 mm Hydrus			
L	Length of device in SC	7.2 mm	Yuan et al. (2016)
L_w	Length of window region	1.1 mm	Yuan et al. (2016)
L_s	Length of spine region	0.9 mm	Yuan et al. (2016)
L_{in}	Length of inlet spine region	1.1 mm	Yuan et al. (2016)
N_w	Number of windows	3	Yuan et al. (2016)
A_w	Area of window region	17553 μm^2	Yuan et al. (2016)
A_s	Area of spine region	22955 μm^2	Yuan et al. (2016)
A_{in}	Area of inlet spine region	29841 μm^2	Yuan et al. (2016)
w	Width of device	292 μm	FDA product insert
h_w	Height of window portion	76.5 μm	$\frac{4A_w}{\pi w}$
h_s	Height of spine portion	100.0 μm	$\frac{4A_s}{\pi w}$
h_{in}	Height of inlet spine region	130.1 μm	$\frac{4A_{in}}{\pi w}$
iStent *inject*			
L	Length of device in SC	230 μm	Glaukos (2018)
w	Diameter of device outlets	50 μm	Glaukos (2018)
h	Same as w for the iStent	50 μm	Glaukos (2018)
d_{in}	Diameter of inlet	80 μm	Glaukos (2018)
h_d	Height of device in SC	150 μm	Analysis of device photo (Glaukos, 2018)

2.2. Model for surgically treated eye

Several surgical methods for lowering outflow resistance in glaucoma were modeled. Trabeculotomy or trabeculectomy, in which trabecular meshwork and the inner wall of Schlemm canal are either cut or removed in a portion of the eye, respectively, were modeled by removing the TM and SC resistors in the region where the surgery was performed. The effects of varying degrees of trabeculotomy in enucleated eyes were examined using the model at pressures of either 7 or 25 mm Hg and comparing to results of corresponding perfusion experiments by Rosenquist et al. (1989). In addition to traditional trabeculotomy, the model was also compared with several minimally invasive approaches to trabeculotomy and trabeculectomy. The Trabectome (NeoMedix, Tustin, CA) is a device for performing ab interno partial trabeculectomy, which allows the surgeon to ablate between 90° and 120° of the trabecular meshwork through a small corneal incision (Vold, 2011). The effect of the Trabectome was modeled by removing the trabecular meshwork and Schlemm canal resistors in a 90°–120° region of Schlemm canal. Predicted IOP was determined for a number of trabeculotomies, randomly varying the length from 90 to 120° as well as the location around the canal. These predicted IOPs were then used to calculate a mean and standard deviation. Gonioscopy-assisted transluminal trabeculotomy (GATT) is a minimally invasive method for performing 360° ab interno trabeculotomy (Grover et al., 2014). The TRAB360 (Sight Sciences, Menlo Park, CA) is a device which can perform 360° ab interno trabeculotomy using a method similar to GATT (Sarkisian et al., 2019). Both GATT and the TRAB360 are modeled by removing all TM and SC resistors, leaving only the CCs.

Additionally, three trabecular bypass stents were modeled. The

Table 3
Baseline resistance for clinical studies.

Treatment	Study	Mean Baseline IOP (mmHg)	R_{TM} (mmHg/μL/min)
Trabectome	Vold (2011)	23.6	5.58
GATT	Grover et al. (2014)	25.6	6.42
TRAB360	Sarkisian et al. (2019)	23.7	5.62
iStent	Katz et al. (2015)	25	6.16
8 mm Hydrus	Fea et al. (2017)	23.1	5.42
iStent *inject*	Fea et al. (2014)	25.2	6.25

iStent (Glaukos Corp., Laguna Hills, CA), a 1 mm long titanium microstent (Fig. 3A) (Hunter et al., 2014); the 8 mm Hydrus Microstent (Ivantis Inc., Irvine, CA), an 8 mm scaffold made from nitinol (Fig. 3B) (Grierson et al., 2015; Yuan et al., 2016); and the iStent *inject*, the smaller, second generation of the iStent (Fig. 3C) (Bahler et al., 2012). When the iStent *inject* is used clinically, almost always two of the stents rather than one are implanted 1–3 clock-hours apart. For our study comparing model predictions to clinical results (Fig. 8), two iStent *injects* were modeled as being 2 clock hours apart from one other. In a study modeling how stent separation affects IOP reduction (Fig. 11), the distance between iStent *injects* was varied from 1 to 6 clock hours.

Trabecular bypass stents have an opening, referred to as the inlet, that connects the anterior chamber to the lumen of Schlemm canal. This opening is modeled exactly the same as trabeculotomy, i.e. by removing the trabecular meshwork resistors where the stent is placed. Second, as these stents dilate Schlemm canal to well above its natural undeformed height, this part of the stent is modeled by holding the canal (at the locations filled by the stent) at a height determined by the size of the stent. This dilation is reflected in the model by replacing h and W in equation (3) with the corresponding heights and widths listed in Table 2 for each device. In the iStent and iStent *inject*, the portion of the stent dilating the canal also blocks flow through the trabecular meshwork, so no flow is allowed to enter this part of the canal through the TM resistors. In the Hydrus, however, there are "window" regions, which allow flow to enter through the trabecular meshwork, but still keep Schlemm canal dilated, and "spine" regions which block flow through the trabecular meshwork.

Similar to the modeling studies of the Trabectome, a number of simulations were run randomly varying the location where each stent was placed around the canal, and the resulting IOPs were then used to calculate a mean and standard deviation for the predicted postoperative IOP. The resulting variability represents the variability due to the location of surgical intervention relative to the collector channel ostia.

Both the iStent and iStent *inject* are bidirectional bypasses, meaning that once aqueous humor enters through the inlet, it can travel in either direction through Schlemm canal. This is reflected in the model by allowing flow to travel in either direction from the inlet. The Hydrus, on the other hand, is unidirectional, only allowing flow to travel in the direction of the scaffold from the inlet.

We excluded from our modeling any clinical studies that included phacoemulsification due to the IOP-lowering effect of cataract surgery (Mansberger et al., 2012).

2.3. Model for glaucomatous eye

In order to accurately compare the model predictions for treatments to the results of clinical studies, baseline IOPs from the studies must be matched by the model. Since the source of increased outflow resistance in primary open-angle glaucoma is generally thought to be in the trabecular meshwork (and/or inner wall of Schlemm canal), the TM resistance was the parameter used to match clinical baseline IOP. Episcleral venous pressure was assumed to be 8 mmHg (Podos et al., 1968) for all studies compared. The values of R_{TM} used for each study and device are shown in Table 3. The aqueous flowrate passing through the outflow pathway was assumed to be 2 μL/min (Brubaker, 1982) for all simulations. The R_{TM} values shown in Table 3 were determined by adjusting R_{TM} so that the model returned the same baseline IOP as was reported in the corresponding clinical study assuming the conditions outlined above.

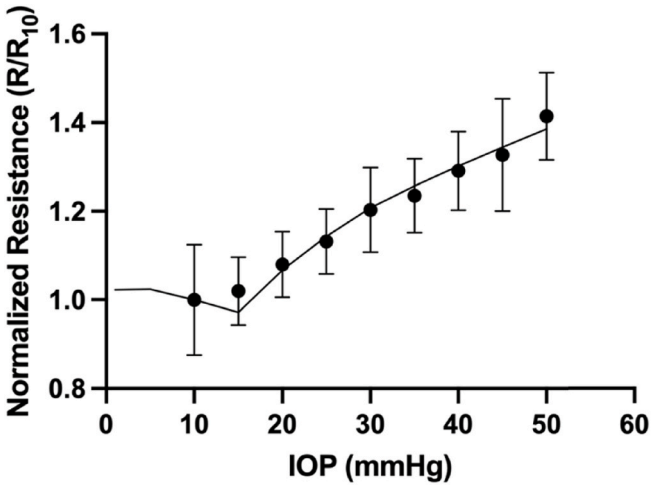

Fig. 4. Flow resistance of enucleated human eyes (normalized to the mean value at 10 mm Hg) as a function of IOP (Brubaker, 1975). The solid line is the best fit of the baseline model to the data (see text). Error bars are standard errors of the experimental measurements.

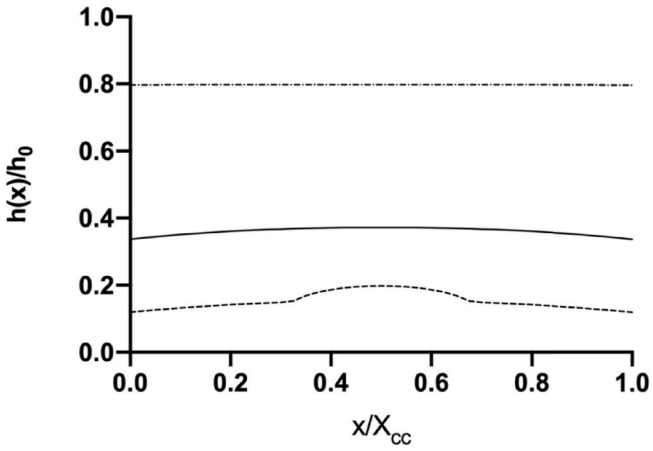

Fig. 5. Model predictions for the normalized height of Schlemm canal, $h(x)/h_0$, as a function of the distance from a collector channel, normalized by the distance between adjacent collector channels, X_{CC}. The two collector channels are located at $x/X_{CC} = 0$ and $x/X_{CC} = 1$. The canal height is shown for an enucleated eye at IOP = 5 mmHg (dot-dashed line), 15 mm Hg (solid line) and 30 mm Hg (dashed line). h_0 is the undeformed canal height (at IOP = 0 mmHg).

3. Results

3.1. Model validation

Fig. 4 shows the best fit of the model to data for flow resistance as a function of pressure in enucleated human eyes (Brubaker, 1975). The small decrease in outflow resistance between 5 and 15 mmHg in the model is due to decreasing CC resistance with increasing IOP; the increasing resistance at higher pressures is due to collapse of Schlemm canal. This small decrease in resistance is not seen in the experiment

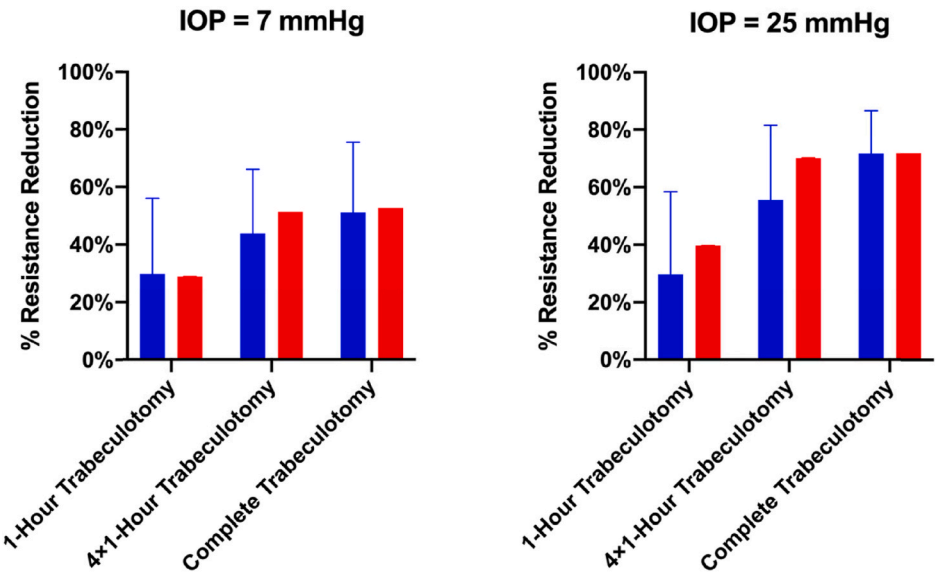

Fig. 6. Model predictions (red) of resistance reduction for varying degrees of trabeculotomy in enucleated eyes as compared with experimental results (blue) (Rosenquist et al., 1989). Error bars are standard deviations. (For interpretation of the references to color in this figure legend, the reader is referred to the Web version of this article.)

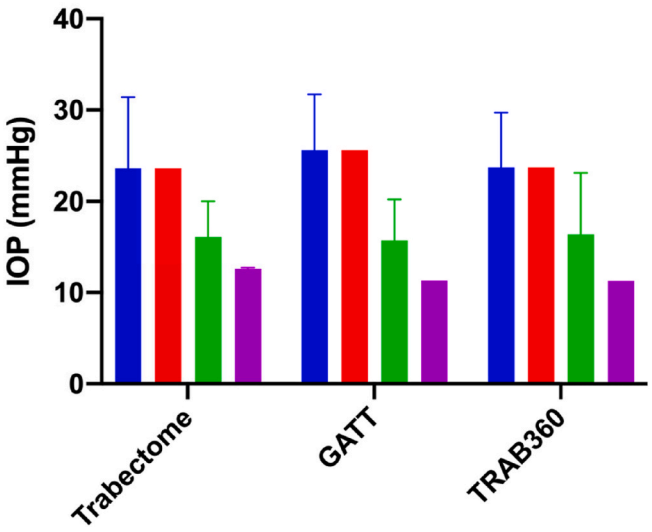

Fig. 7. Comparison of model predictions for IOP reduction with results of clinical studies (Grover et al., 2014; Sarkisian et al., 2019; Vold, 2011) for ab interno trabeculotomy procedures. In all three clinical studies, IOP reducing medication was uncontrolled at both the baseline and 12-month IOP measurements. Baseline pressures for the clinical studies are shown blue and 12-month post-operative results are shown in green; baselines for the model (red) are the same as for the model as for the clinical studies, and model predictions for effect of the procedures are shown in purple. Error bars are standard deviations. (For interpretation of the references to color in this figure legend, the reader is referred to the Web version of this article.)

data likely due to natural variability in the human outflow system, as reflected in the measured standard deviations.

The model for canal collapse was further validated by comparing the height distributions in Schlemm canal, shown in Fig. 5, with observations of canal collapse at different pressures. Johnstone and Grant (1973) examined Schlemm canal in enucleated human eyes at several levels of IOP. At an IOP of 5 mmHg, they observed the canal to be open, consistent with the model's prediction that the canal is at ~80% of its undeformed height. At 15 mmHg, Johnstone and Grant observed the canal to be in a transition between collapsed and uncollapsed states. This

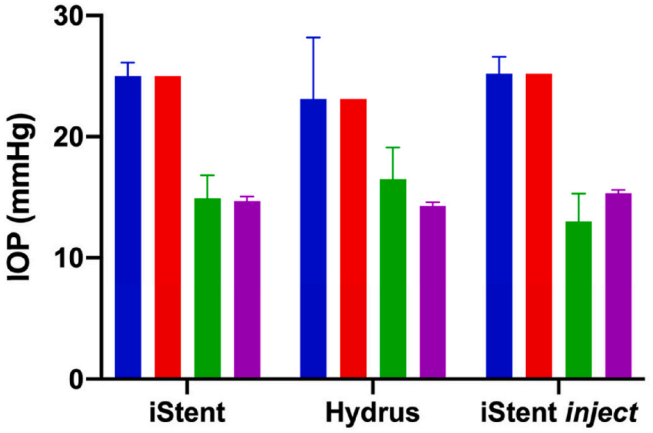

Fig. 8. Comparison of model predictions for IOP reduction with results of clinical studies (Fea et al., 2014, 2017; Katz et al., 2015) for trabecular bypass stents. In Katz et al. (2015) (iStent), patients underwent medication washout prior to both the baseline and 12-month IOP measurements. In Fea et al. (2017) (Hydrus), IOP reducing medication was uncontrolled at both the baseline and 12-month measurements. In Fea et al. (2014) (iStent inject), patients underwent medication washout prior to the baseline measurement, however, many patients resumed medication prior to the 12-month measurement. Legend is same as Fig. 7.

agrees with the model's prediction that the canal is collapsed down to ~35% of its undeformed height but is not quite collapsed enough for the septae to begin supporting the canal. Finally, at 30 mmHg, they observed the canal to be fully collapsed, consistent with the model's prediction that ~70% of the canal is collapsed and supported by the septae at this pressure.

3.2. Simulation of trabeculotomy and trabeculectomy

Model predictions of percent reduction of outflow resistance after 1-h, 4 × 1-h, and complete 12-h trabeculotomy at constant IOPs of 7 mmHg and 25 mmHg were compared with the results of corresponding constant pressure perfusion experiments in enucleated human eyes (Rosenquist et al., 1989). The resulting resistance data is shown in Fig. 6.

The model predictions are generally good, although they somewhat overpredict the effect of partial trabeculotomy at 25 mmHg. Interestingly, the model predicts almost no difference in resistance between the 4 × 1-h and complete 12-h trabeculotomies, which is not observed experimentally. This is likely due to the fact that the model does not account for weakening of the trabecular meshwork caused by the procedure that would be expected to increase the resistance in the 4 × 1-h trabeculotomy due to increased Schlemm canal collapse.

Model predictions for the effects of Trabectome, GATT and TRAB360 procedures on IOP as compared to clinical results are shown in Fig. 7. Agreement between the model and clinical results are also generally good, although the model overpredicts the success of the procedures. In these cases, the overpredicted pressure reduction is due, at least in part, to fewer IOP-reducing medications taken by the patients following successful surgery (Grover et al., 2014; Sarkisian et al., 2019; Vold, 2011). As well, the model does not account for other surgical factors such as inflammation, bleeding/hyphema and the release of debris that will affect flow into the collector channels that have been unroofed by the trabeculectomy procedures.

3.3. Simulation of stents

Model predictions for the effects of inserting stents into Schlemm canal are shown in Fig. 8. Similar to the predictions of trabecular surgery described above, the model showed good agreement with clinical results 12 months after implantation of the stents but somewhat overpredicted procedure success for the Hydrus. This overprediction is, again, likely due to the fact that patients were taking fewer IOP reducing medications at 12 months than at the baseline measurement (Fea et al., 2017). The agreement between the model predictions and clinical results was good for the iStent. For the iStent *injects*, the model slightly underpredicts the success of the procedure. This underprediction is likely due to the fact that patients in this study underwent medication washout for the baseline IOP measurement, but not for the IOP measurement at 12 months (Fea et al., 2014).

4. Discussion

The goal of minimally invasive glaucoma surgery is to adequately lower IOP while minimizing surgical trauma to the anterior segment of the eye. Accurate estimation of the effect of surgical procedures on outflow resistance can greatly facilitate achievement of this goal. The model we have developed treats the outflow pathway as a network of resistors and uses circuit theory to predict the result of removing various resistors from the network.

Predictions from the model gave generally good agreement with results from a variety of surgical procedures although the predicted reductions in patients tended to be greater than those seen clinically (Figs. 7 and 8). A likely explanation for at least part of this discrepancy is that medication was not a controlled variable in the clinical trials of the ab interno trabeculotomy. As patients' pressure controlimproved following surgery, their pressure reducing medication was reduced, likely offsetting some of the IOP reduction from the surgery (Grover et al., 2014; Sarkisian et al., 2019; Vold, 2011); simulations of reductions in topical aqueous suppressants using the resistor model confirm this speculation (data not shown). It is also important to note that the clinical results that we compared our model predictions to are for a time point 12 months after the procedure during which time healing would have occurred that could have lessened the effect of the procedure.

All of the IOP reducing procedures modeled here involve some form of opening into Schlemm canal, thus allowing direct communication between the anterior chamber and the canal. If Schlemm canal had no resistance to circumferential flow, then only a small opening in the inner wall would be required to reduce the outflow resistance to that of the collector channels. However, due to the flow resistance that the canal presents, procedures that opened only part of the canal (limited trabeculotomy or use of stents) fall short of this result. Fig. 9 shows the predicted flow distribution through the collector channels after a 1-h trabeculotomy at constant flow for a glaucomatous eye (R_{TM} increased from normal eye by 3-fold), with substantially increased flow to collector channels within approximately 1.5 clock hours of the trabeculotomy site, while those further away carry equal or less flow than they would without surgery.

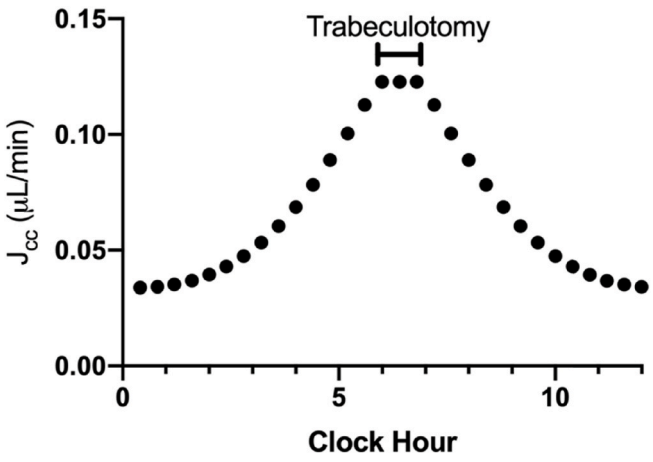

Fig. 9. Distribution of flow (J_{cc}) through collector channels with 1-h trabeculotomy (marked by capped line) in a glaucomatous eye with R_{TM} = 6 mmHg/μL/min and a constant flow of 2 μL/min.

Trabecular bypass stents lower outflow resistance by providing direct access from the anterior chamber to Schlemm canal as well as dilating parts of Schlemm canal to well above its undeformed height. Dilation of Schlemm canal effectively eliminates circumferential resistance in the region occupied by the stent. Similar to trabeculotomy, the collector channels in the region occupied by a stent as well as approximately 1.5 clock hour past the open ends of a stent carry the bulk of the flow, while those further away carry less flow.

Our model predicted a somewhat larger pressure reduction than was seen clinically (at 12 months) for the Hydrus (Fig. 8). As with the ab interno trabeculotomies, this discrepancy can be partly explained by the fact that medication was not a controlled variable in this clinical study of the Hydrus (Fea et al., 2017). The model predictions matched well for the iStent. For the iStent *injects*, the model slightly underpredicted the IOP reduction seen clinically (Fig. 8). Similar to the Hydrus and ab interno trabeculotomies, medication is a confounding variable in this clinical study of the iStent *inject*. Patients underwent medication washout prior to their baseline IOP measurement, however many patients resumed some medication prior to their IOP measurement at 12 months, leading to further reduction of IOP (Fea et al., 2014). This underprediction may also be due to another mechanism by which the stents could reduce outflow resistance. By expanding Schlemm canal to well above its undeformed height, resistance to circumferential flow is effectively eliminated not only within the stent but likely beyond the end of the stent, such that collector channels in this dilated region can carry additional flow. This is consistent with observations from scanning electron microscopy studies that Schlemm canal is dilated past the region dilated by the stent (Bahler et al., 2012; Johnstone et al., 2014), although this effect was not included in the model results presented. This dilation would have the largest effect for the iStent *inject*, because two stents are placed into the canal.

The model predicts a 4 × 1-h trabeculotomy to be equally effective as complete trabeculotomy, in contrast to experimental results indicating a meaningful difference in resistance between the two procedures. This is likely due to the model not accounting for any meshwork weakening effects that the procedure might have, which would increase the resistance in the 4 × 1-h trabeculotomy (Fig. 6). The 4x1-hour trabeculotomy

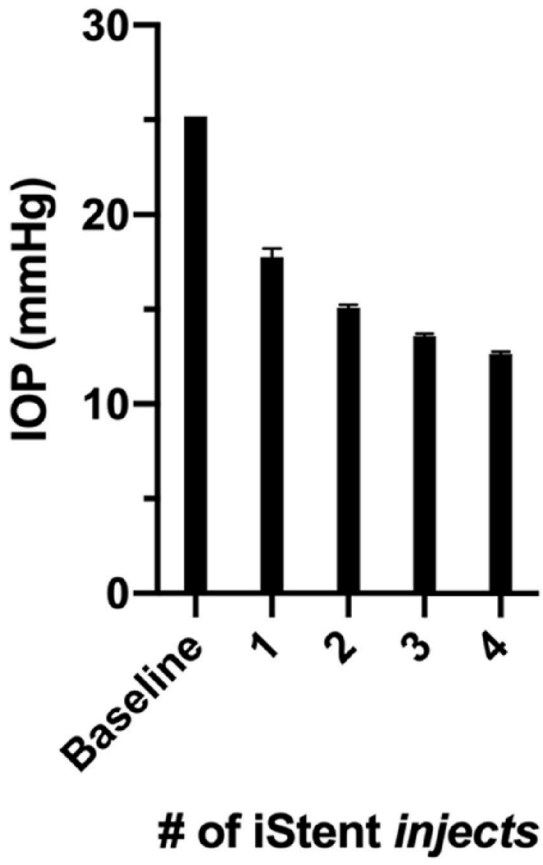

Fig. 10. Comparison of predicted IOP using one, two, three, and four iStent *injects* inserted into Schlemm canal 90° apart, from a baseline pressure of 25 mm Hg. Error bars are standard deviations.

would create eight points of direct communication between the anterior chamber and Schlemm canal, but these openings could be partly obstructed by debris and collapse of the canal structure, thus leading to the over-prediction of the resistance reduction by the model. Similarly, the model prediction (Fig. 7) for pressure reduction following use of the Trabectome, which removes a segment of the trabecular meshwork, was greater than seen clinically, although this was likely due in large part to reduction in pressure-lowering medications take by the patients following successful pressure reduction (Vold, 2011). Future work could model the reduction in IOP when combining a MIGS procedure with reduction in medications by altering the rate of aqueous production in the model predictions. Topical aqueous suppressants usually reduce IOP (and presumably aqueous production) by 20–25% when used as monotherapy, but when used in combination the effect is not additive. As such, the reduction in aqueous production when reducing medical therapy from multiple drugs is harder to model accurately.

When the trabecular meshwork is fully removed in a complete 360° trabeculotomy (GATT and TRAB360), the model predicts that the resistance to outflow should be reduced to that of the collector channels. However, the model overestimated the IOP reduction for these ab interno trabeculotomy procedures (Fig. 7) suggesting that these procedures do not eliminate all trabecular meshwork and Schlemm canal flow resistance. This can again be partly explained by the reduction in pressure-lowering medications, but another consideration is the mechanism of action for GATT trabeculotomy, which is to tear open the trabecular meshwork rather than remove it. The flap of trabecular meshwork left behind after surgery is commonly referred to as a trabecular shelf (Grover et al., 2014). Clinically, the presence of a trabecular shelf could be associated with a positive surgical outcome, as the flap of trabecular meshwork may attach to the iris and hold the canal

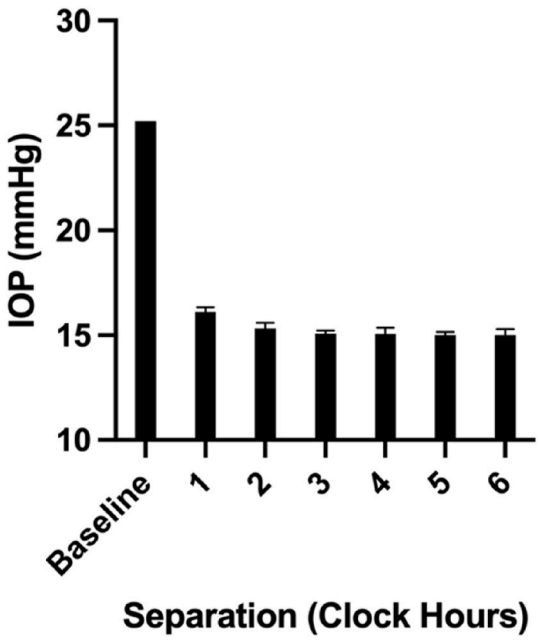

Fig. 11. Predicted IOP following implantation of two iStent *injects* separated by 1–6 clock hours compared to the preoperative baseline of 25.2 mm Hg. Error bars are standard deviations.

open; however, the presence of the torn trabecular meshwork debris after GATT may add flow resistance by blocking the collector channels.

In a previous study modeling trabecular bypass stents, Yuan et al. (2016) argued that a further mechanism by which Schlemm canal stents lower outflow resistance is by dilation of the collector channel ostia. While this assumption worked well for the 8 mm Hydrus, with their model predicting a 35% IOP reduction from a 25 mmHg baseline similar to the 28% reduction from a 23.1 mmHg baseline found in a clinical study by Fea et al. (2017), they greatly underestimated the IOP reduction brought on by the iStent, predicting only a 16% reduction from a 25 mmHg baseline, as compared to a 40% reduction seen in a clinical study (Katz et al., 2015). Collector channel ostia have large openings (Bentley et al., 2016), and so it is hard to understand how dilation at just the ostia would significantly alter their resistance. Furthermore, scanning electron microscopy studies have found that Schlemm canal scaffolds like the 8 mm Hydrus may even have the potential to occlude some collector channel ostia, rather than dilate them (Johnstone et al., 2014).

We view the utility of the model we have developed not primarily as one of verifying the results of previous experimental studies, but instead of prospectively predicting the usefulness of procedures for lowering outflow resistance. To demonstrate its utility, we performed three hypothetical analyses: first we consider the progressive lowering of IOP that would be expected if one to four iStent *injects* were inserted into Schlemm canal 90° apart; as a second example, we investigate how the IOP reduction from two iStent *injects* is affected by the separation between the two devices implanted; finally, we ask how much the Hydrus efficiency would be increased if it were made bi-directional. The IOP reductions reported in these hypothetical scenarios use the baseline IOPs from the iStent *inject* and Hydrus clinical studies, respectively. Note that these are only model predictions, as we are unaware of studies that have investigated these questions experimentally.

Predictions of the IOP reduction when one, two, three, and four iStent *injects* are implanted 90° apart is shown in Fig. 10. IOP is reduced the most by the first device implanted, and the addition of each new device lowers IOP further, but to a lesser degree.

Fig. 11 shows the IOP reduction when two iStent *injects* are implanted 1–6 clock hours apart from each other. IOP reduction is improved by each additional clock hour of separation; however, the

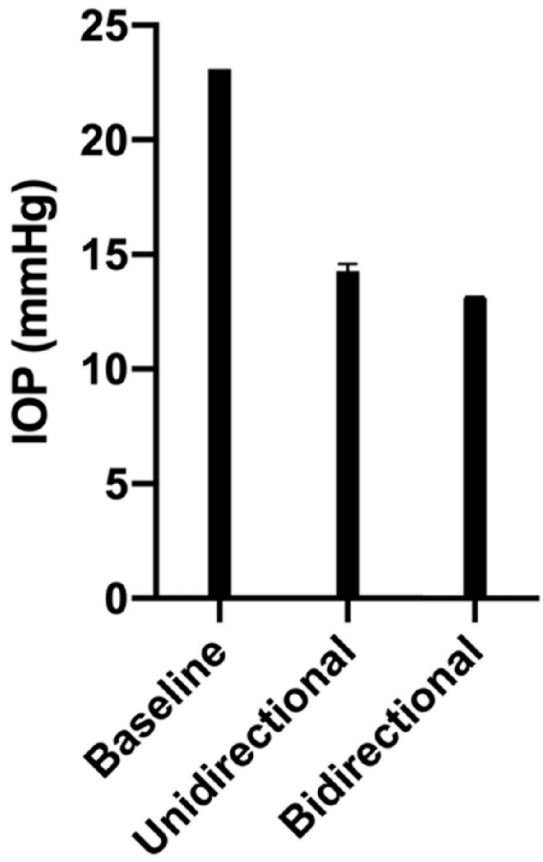

Fig. 12. Comparison of predicted IOP between the unidirectional Hydrus stent with a hypothetical bi-directional version of the Hydrus stent from a baseline of 23 mm Hg. Error bars are standard deviations.

impact on IOP is minimal beyond 3 clock hours of separation. This is a reflection of the findings described above that stents increase flow through collector channels up to 1.5 clock hours beyond the region occupied by the stent. When the stents are placed within 3 clock hours of each other, the 1.5 clock hour regions overlap, decreasing the number of collector channels which carry excess flow. Separating the stents by three or more clock hours ensures that there is no overlap of the regions of Schlemm canal affected by the two stents.

Fig. 12 shows predictions of the potential increased pressure reduction of a bi-directional Hydrus. Making the Hydrus bi-directional decreases IOP by an additional 5% as compared with a unidirectional Hydrus.

The effect on outcome of the relative location of collector channels is another parameter that could be examined using our model. An optimally located trabeculotomy might be performed on the region of Schlemm canal containing the highest concentration of patent collector channel entrances. Similarly, an optimally placed stent maximizes the number of patent collector channel entrances in the stent region and surrounding 2–3 clock hours. The model we have developed could be used to predict where these optimal locations might be. In order to achieve this, recent advances in imaging technology for visualizing Schlemm canal and collector channels might be utilized (Ren et al., 2011). In all of the simulations discussed here, a uniform collector channel distribution was used, however in the human eye, collector channels have neither uniform size nor location (Hann et al., 2011). IOP reductions from both ab interno trabeculotomies and trabecular bypass stents in an eye with nonuniform collector channels were determined and are included in the Supplementary Information. Altering the collector channel distribution had minimal effect on the average IOP reductions, but greatly increased the variability due to the location of the surgical interventions.

The aqueous outflow human model developed and validated in this study for surgical alterations to the conventional outflow pathway at the level of the trabecular meshwork can guide the development of new surgical devices and procedures for the treatment of glaucoma. Implants can be customized according to the desired degree of IOP reduction either through the number of devices implanted or their circumferential spacing in the angle. Procedures that remove trabecular meshwork can be customized in terms of the extent of tissue removal to balance the targeted IOP reduction with the potential for complications resulting from excessive tissue disruption. This modeling will optimize procedures and improve patient outcomes in glaucoma surgery that alters the aqueous outflow system.

Funding

This work was supported by NIH [1R01EY019696].

Acknowledgements

We gratefully acknowledge useful discussions with Prof. Roger Kamm of MIT.

Supplementary data

Supplementary data to this article can be found online at https://doi.org/10.1016/j.exer.2021.108620.

Appendix A

Relationship between canal height and IOP when the canal is collapsed. In enucleated human eyes, the total outflow resistance has been observed to vary linearly with IOP (Brubaker, 1975) for IOP greater than approximately 15 mmHg, at which point Schlemm canal is observed to be partially collapsed in enucleated eyes (with zero episcleral venous pressure) (Johnstone and Grant, 1973). We assume that in this pressure range, the increasing flow resistance is largely due to progressively increasing Schlemm canal collapse. As such, the resistance in Schlemm canal (R_{SC}) must vary linearly with IOP.

$$\frac{\partial R_{SC}}{\partial IOP} \propto constant \tag{A4}$$

Equation (3) shows that R_{SC} varies with respect to canal height as

$$R_{SC} \sim \frac{1}{h^3} \tag{A5}$$

and thus we conclude that:

$$\frac{1}{h^4}\frac{\partial h}{\partial IOP} \propto constant \tag{A6}$$

or,

$$IOP \sim \frac{1}{h^3} \tag{A7}$$

This relationship applies to enucleated eyes in which episcleral venous pressure is zero. In live eyes, this relationship becomes

$$IOP - P_{SC} \sim \frac{1}{h^3} \tag{A8}$$

Solving for h and by introducing the constants h_s and K_S, equation (5) results.

References

Bahler, C.K., Hann, C.R., Fjield, T., Haffner, D., Heitzmann, H., Fautsch, M.P., 2012. Second-generation trabecular meshwork bypass stent (iStent inject) increases outflow facility in cultured human anterior segments. Am. J. Ophthalmol. 153, 1206–1213.

Bentley, M.D., Hann, C.R., Fautsch, M.P., 2016. Anatomical variation of human collector channel orifices. Invest. Ophthalmol. Vis. Sci. 57, 1153–1159.

Brubaker, R.F., 1975. The Effect of Intraocular Pressure on Conventional Outflow Resistance in the Enucleated Human Eye. undefined.

Brubaker, R.F., 1982. The flow of aqueous humor in the human eye. Trans. Am. Ophthalmol. Soc. 80, 391–474.

de Kater, A.W., Melamed, S., Epstein, D.L., 1989. Patterns of aqueous humor outflow in glaucomatous and nonglaucomatous human eyes: a tracer study using cationized ferritin. Arch. Ophthalmol. 107, 572–576.

Ethier, C.R., Read, A.T., Chan, D., 2004. Biomechanics of Schlemm's canal endothelial cells: influence on F-actin architecture. Biophys. J. 87, 2828–2837.

Fea, A.M., Ahmed, I.I.K., Lavia, C., Mittica, P., Consolandi, G., Motolese, I., Pignata, G., Motolese, E., Rolle, T., Frezzotti, P., 2017. Hydrus microstent compared to selective laser trabeculoplasty in primary open angle glaucoma: one year results. Clin. Exp. Ophthalmol. 45, 120–127.

Fea, A.M., Belda, J.I., Rękas, M., Jünemann, A., Chang, L., Pablo, L., Voskanyan, L., Katz, L.J., 2014. Prospective unmasked randomized evaluation of the iStent inject (®) versus two ocular hypotensive agents in patients with primary open-angle glaucoma. Clin. Ophthalmol. 8, 875–882.

Gedde, S.J., Schiffman, J.C., Feuer, W.J., Herndon, L.W., Brandt, J.D., Budenz, D.L., 2012. Treatment outcomes in the tube versus trabeculectomy (TVT) study after five years of follow-up. Am. J. Ophthalmol. 153, 789–803 e782.

Glaukos, iStent inject, in: GLKOS-15559-Single-iStent.jpg (Ed.). Glaukos, glaukos.com.

Glaukos, 2018. GLAUKOS ® CORPORATION ISTENT Inject ® TRABECULAR MICRO-BYPASS SYSTEM PMA P170043.

Grierson, I., Saheb, H., Kahook, M.Y., Johnstone, M.A., Ahmed, I.I.K., Schieber, A.T., Toris, C.B., 2015. A Novel schlemm's canal scaffold: histologic observations. J. Glaucoma 460–468.

Grover, D.S., Godfrey, D.G., Smith, O., Feuer, W.J., Montes de Oca, I., Fellman, R.L., 2014. Gonioscopy-assisted transluminal trabeculotomy, ab interno trabeculotomy: technique report and preliminary results. Ophthalmology 121, 855–861.

Gulati, V., Fan, S., Hays, C.L., Samuelson, T.W., Ahmed, I.I.K., Toris, C.B., 2013. A Novel 8-mm schlemm's canal scaffold reduces outflow resistance in a human anterior segment perfusion model. Investigative Opthalmology & Visual Science 54, 1698.

Hann, C.R., Bentley, M.D., Vercnocke, A., Ritman, E.L., Fautsch, M.P., 2011. Imaging the aqueous humor outflow pathway in human eyes by three-dimensional micro-computed tomography (3D micro-CT). Exp. Eye Res. 92, 104–111.

Hoffmann, F., Dumitrescu, L., 1971. Schlemm's canal under the scanning electron microscope. Ophthalmic Res. 2, 37–45.

Hunter, K.S., Fjield, T., Heitzmann, H., Shandas, R., Kahook, M.Y., 2014. Characterization of micro-invasive trabecular bypass stents by ex vivo perfusion and computational flow modeling. Clin. Ophthalmol. 8, 499–506.

Johnson, M., 2006. What controls aqueous humour outflow resistance? Exp. Eye Res. 82, 545–557.

Johnson, M., Kamm, R.D., 1983. The role of Schlemm's canal in aqueous outflow from the human eye. Invest. Ophthalmol. Vis. Sci. 24, 320–325.

Johnson, M., McLaren, J.W., Overby, D.R., 2017. Unconventional aqueous humor outflow: a review. Exp. Eye Res. 158, 94–111.

Johnstone, M.A., Grant, W.G., 1973. Pressure-dependent changes in structures of the aqueous outflow system of human and monkey eyes. AJO (Am. J. Ophthalmol.) 75, 365–383.

Johnstone, M.A., Saheb, H., Ahmed, I.I.K., Samuelson, T.W., Schieber, A.T., Toris, C.B., 2014. Effects of a Schlemm canal scaffold on collector channel ostia in human anterior segments. Exp. Eye Res. 119, 70–76.

Kaplowitz, K., Schuman, J.S., Loewen, N.A., 2014. Techniques and outcomes of minimally invasive trabecular ablation and bypass surgery. BJO (Br. J. Ophthalmol.) 98, 579–585.

Katz, L.J., Erb, C., Carceller, G.A., Fea, A.M., Voskanyan, L., Wells, J.M., Giamporcaro, J. E., 2015. Prospective, randomized study of one, two, or three trabecular bypass stents in open-angle glaucoma subjects on topical hypotensive medication. Clin. Ophthalmol. 9, 2313–2320.

Magazine, M.P.O., 2018. Study: Glaukos iStent Trabecular Micro-bypass Stent Reduces IOP. Lowers Medication Burden.

Mansberger, S.L., Gordon, M.O., Jampel, H., Bhorade, A., Brandt, J.D., Wilson, B., Kass, M.A., 2012. Reduction in intraocular pressure after cataract extraction: the ocular hypertension treatment study. Ophthalmology 119, 1826–1831.

Moses, R.A., 1977. The effect of intraocular pressure on resistance to outflow. Surv. Ophthalmol. 22, 88–100.

Podos, S.M., Minas, T.F., Macri, F.J., 1968. A new instrument to measure episcleral venous pressure: Comparison of normal eyes and eyes with primary open-angle glaucoma. JAMA Ophthalmology 80, 209–213.

Ren, J., Gille, H.K., Wu, J., Yang, C., 2011. Ex vivo optical coherence tomography imaging of collector channels with a scanning endoscopic probe. Invest. Ophthalmol. Vis. Sci. 52, 3921–3925.

Richter, G.M., Coleman, A.L., 2016. Minimally invasive glaucoma surgery: current status and future prospects. Clin. Ophthalmol. 10, 189–206.

Rosenquist, R., Epstein, D., Melamed, S., Johnson, M., Grant, W.M., 1989. Outflow resistance of enucleated human eyes at two different perfusion pressures and different extents of trabeculotomy. Curr. Eye Res. 8, 1233–1240.

Sarkisian, S.R., Mathews, B., Ding, K., Patel, A., Nicek, Z., 2019. 360° ab-interno trabeculotomy in refractory primary open-angle glaucoma. Clin. Ophthalmol. 13, 161–168.

Vold, S.D., 2011. Ab interno trabeculotomy with the trabectome system: what does the data tell us? Int. Ophthalmol. Clin. 51, 65–81.

Weinreb, R.N., Aung, T., Medeiros, F.A., 2014. The pathophysiology and treatment of glaucoma: a review. J. Am. Med. Assoc. 311, 1901–1911.

White, F.M., Corfield, I., 2006. Viscous Fluid Flow. McGraw-Hill, New York.

Yuan, F., Schieber, A.T., Camras, L.J., Harasymowycz, P.J., Herndon, L.W., Rand Allingham, R., 2016. Mathematical modeling of outflow facility increase with trabecular meshwork bypass and schlemm canal dilation. J. Glaucoma 25, 355–364.

Zhou, J., Smedley, G.T., 2006. Trabecular bypass: effect of Schlemm canal and collector channel dilation. J. Glaucoma 15, 446–455.